



**HAL**  
open science

## Multimodal neuroimaging correlates of spectral power in NREM sleep delta sub-bands in cognitively unimpaired older adults

Pierre Champetier, Claire André, Stéphane Rehel, Valentin Ourry, Brigitte Landeau, Florence Mézenge, Daniel Roquet, Denis Vivien, Vincent de La Sayette, Gaël Chételat, et al.

### ► To cite this version:

Pierre Champetier, Claire André, Stéphane Rehel, Valentin Ourry, Brigitte Landeau, et al.. Multimodal neuroimaging correlates of spectral power in NREM sleep delta sub-bands in cognitively unimpaired older adults. *Sleep*, 2024, pp.zsae012. 10.1093/sleep/zsae012 . inserm-04452472

**HAL Id: inserm-04452472**

**<https://inserm.hal.science/inserm-04452472v1>**

Submitted on 12 Feb 2024

**HAL** is a multi-disciplinary open access archive for the deposit and dissemination of scientific research documents, whether they are published or not. The documents may come from teaching and research institutions in France or abroad, or from public or private research centers.

L'archive ouverte pluridisciplinaire **HAL**, est destinée au dépôt et à la diffusion de documents scientifiques de niveau recherche, publiés ou non, émanant des établissements d'enseignement et de recherche français ou étrangers, des laboratoires publics ou privés.

# Multimodal neuroimaging correlates of spectral power in NREM sleep delta sub-bands in cognitively unimpaired older adults

Pierre Champetier\*<sup>1,2</sup>, Claire André\*<sup>1</sup>, Stéphane Rehel<sup>1,2</sup>, Valentin Ourry<sup>1,2</sup>, Brigitte Landeau<sup>1</sup>,  
Florence Mézenge<sup>1</sup>, Daniel Roquet<sup>1</sup>, Denis Vivien<sup>1,3</sup>, Vincent de La Sayette<sup>4</sup>, Gaël Chételat<sup>1</sup>,  
Géraldine Rauchs<sup>1</sup>, on behalf of the Medit-Ageing Research Group.

<sup>1</sup> Normandie Univ, UNICAEN, INSERM, U1237, PhIND "Physiopathology and Imaging of Neurological Disorders", NeuroPresage team, Institut Blood and Brain @ Caen-Normandie, GIP Cyceron, 14000 Caen, France.

<sup>2</sup> Normandie Univ, UNICAEN, PSL Université, EPHE, INSERM, U1077, CHU de Caen, GIP Cyceron, NIMH, 14000 Caen, France.

<sup>3</sup> Département de Recherche Clinique, CHU Caen-Normandie, Caen, France.

<sup>4</sup> Service de Neurologie, CHU de Caen, Caen, France.

\* Equal contribution as first authors.

## **Corresponding author:**

Dr Géraldine Rauchs,  
Inserm U1237, PhIND,  
Team NeuroPresage,  
GIP Cyceron,  
Bd Henri Becquerel, BP 5229,  
14074 Caen cedex 5,  
France

[geraldine.rauchs@inserm.fr](mailto:geraldine.rauchs@inserm.fr)

**Declarations of interest:** none.

## Abstract

**Study Objectives:** In aging, reduced delta power (0.5-4 Hz) during N2 and N3 sleep has been associated with gray matter (GM) atrophy and hypometabolism within frontal regions. Some studies have also reported associations between N2-N3 sleep delta power in specific sub-bands and amyloid pathology. Our objective was to better understand the relationships between spectral power in delta sub-bands during N2-N3 sleep and brain integrity using multimodal neuroimaging.

**Methods:** In-home polysomnography was performed in 127 cognitively unimpaired older adults (mean age  $\pm$  SD: 69.0  $\pm$  3.8 years). N2-N3 sleep EEG power was calculated in delta (0.5-4 Hz), slow delta (0.5-1 Hz) and fast delta (1-4 Hz) frequency bands. Participants also underwent MRI and Florbetapir-PET (early and late acquisitions) scans to assess GM volume, brain perfusion and amyloid burden. Amyloid accumulation over ~21 months was also quantified.

**Results:** Higher delta power was associated with higher GM volume mainly in fronto-cingular regions. Specifically, slow delta power was positively correlated with GM volume and perfusion in these regions, while the inverse association was observed with fast delta power. Delta power was neither associated with amyloid burden at baseline, nor its accumulation over time, whatever the frequency band considered.

**Conclusions:** Our results show that slow delta is particularly associated with preserved brain structure, and highlight the importance of analysing delta power sub-bands to better understand the associations between delta power and brain integrity. Further longitudinal investigations with long follow-ups are needed to disentangle the associations between sleep, amyloid pathology and dementia risk in older populations.

## Keywords

Sleep, Slow-Wave; gray matter; atrophy; amyloid; aging; neuroimaging; EEG.

## Clinical Trial Information

Name: Study in Cognitively Intact Seniors Aiming to Assess the Effects of Meditation Training (Age-Well).

URL: <https://clinicaltrials.gov/ct2/show/NCT02977819?term=Age-Well&draw=2&rank=1>.

See STROBE\_statement\_AGEWELL.doc in supplementary file.

Registration: EudraCT: 2016-002441-36; IDRCB: 2016-A01767-44; ClinicalTrials.gov Identifier: NCT02977819.

## Statement of Significance

In older adults, delta power during N2-N3 sleep is associated with several aspects of brain integrity. Here, we refined spectral analyses by dividing delta power into slow and fast sub-bands and investigated their neural correlates using multimodal neuroimaging. For the first time, we found that delta sub-bands correlate with gray matter volume and brain perfusion in an opposite manner (positively for slow delta, negatively for fast delta), suggesting that associations with delta previously reported were driven by slow delta power. However, we did not observe significant associations with amyloid burden at baseline, or its accumulation over time. Future studies should consider analyze delta power sub-bands separately to investigate the associations with dementia risk.

## Graphical abstract

# Multimodal neuroimaging correlates of spectral power in NREM sleep delta sub-bands in cognitively unimpaired older adults



**N=127 cognitively unimpaired older adults of the Age-Well randomized controlled trial**  
(mean age  $\pm$  SD = 69.0  $\pm$  3.8 years; 63% women; 20.6% amyloid positive)



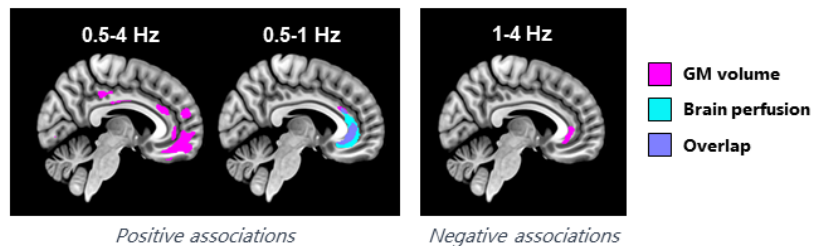
NREM sleep  
delta power



- Gray matter volume
- Brain perfusion
- Amyloid burden
- Amyloid accumulation over ~21 months ( $n=113$ )



Slow (0.5-1 Hz) and fast (1-4 Hz) delta power show opposite associations with fronto-cingulate gray matter volume and perfusion.



Delta power was neither associated with amyloid burden at baseline, nor its accumulation over ~21 months.

## Introduction

Sleep becomes lighter and more fragmented with increasing age [1]. Non-rapid eye movement (NREM) sleep is particularly altered by the aging process, especially N3 sleep which is the deepest NREM sleep stage [2–4]. Delta power (sometimes referred to as delta activity or slow wave activity) corresponds to spectral power computed in the delta frequency band (0.5-4 Hz) on N2 and N3 epochs combined, or N3 only depending on studies. It is a homeostatically-regulated variable considered to reflect neuronal synchronization [5] and has been traditionally used as a proxy of sleep depth [6,7], even this is more and more called into question [8,9]. Delta power during N2 and N3 sleep is known to be reduced in older individuals [2], notably during the first sleep cycles [10]. Interestingly, this age-related decrease in delta power is maximal on frontal derivations [11–14], and has been associated with gray matter (GM) atrophy [12,14–16] and hypometabolism [17] mostly in prefrontal regions.

Beyond normal aging, recent studies suggest that poor sleep quality is associated with Alzheimer's disease pathophysiological processes, including amyloid-beta ( $A\beta$ ) deposition [18,19].  $A\beta$  levels fluctuate with the sleep-wake cycle, increasing during wake periods and decreasing during sleep [20–22]. Indeed, cerebrospinal fluid (CSF) inflows during N3 sleep are thought to play a major role in the clearance of cerebral toxic waste such as  $A\beta$  [23]. Interestingly, CSF inflows are increased during periods with high delta power in both mice [24] and humans [25]. Consistently, recent studies have linked reduced delta power to increases in CSF  $A\beta$  in older adults [26–28], suggesting that the disruption of N3 sleep may affect  $A\beta$  release and/or clearance.

However, few studies have investigated the associations between delta power and amyloid burden measured using Positron Emission Tomography (PET), and these studies have not provided homogeneous results. On the one hand, three studies conducted on partly overlapping samples of 26 to 32 cognitively unimpaired older individuals have linked the power of delta sub-bands during N3 to both prefrontal amyloid burden and accumulation over time [29–31]. More specifically, greater prefrontal amyloid burden was associated to lower relative power in the 0.6-1 Hz frequency band

[29,30] and to higher relative power in the 1-4 Hz frequency band during N3 [29]. Importantly, greater prefrontal amyloid deposition over 3.7 years also correlated with lower relative power in the 0.6-1 Hz frequency band and higher relative power in the 1-4 Hz frequency band [31]. On the other hand, another study conducted in 38 older adults reported no significant association between mean cortical amyloid burden and 1-4.5 Hz power during N2 and N3 combined (referred to as N2-N3 sleep hereafter) [32]. However, decreased 1-2 Hz power was associated with greater cortical amyloid burden, as measured with the averaged standard uptake value ratio over frontal, temporal and parietal regions [32]. Of note, spectral power below 1 Hz was not analyzed in this study due to hardware limitations. Lastly, a more recent study conducted on a younger and larger cohort of 100 healthy adults aged between 50 and 70 years has not revealed any significant association between amyloid burden and delta power sub-bands (or their ratio) during N2-N3 sleep [33]. Overall, the age-related decrease in delta power has been associated with reduced GM volume and metabolism in frontal areas, but the structural and functional correlates of delta power sub-bands have never been investigated so far. In addition, few studies suggest opposite associations between delta power sub-bands and amyloid burden [29,30,32] or accumulation [31] measured using PET.

In this context, our objective was to assess the associations between spectral power in delta sub-bands during both N2-N3 sleep and N3 alone and i) GM volume, perfusion and amyloid burden at baseline, and ii) amyloid accumulation over time in a sample of 127 community-dwelling cognitively unimpaired older adults. We expected these relationships to differ depending on the frequency band considered, such that higher slow delta power would be associated with higher GM volume and brain perfusion, and lower amyloid burden and accumulation over time in frontal regions, whereas higher fast delta power would be associated with GM atrophy, hypoperfusion and greater amyloid burden and accumulation over time in similar regions.

## Materials & Methods

### Participants

One hundred and thirty-seven cognitively unimpaired older participants were enrolled in the baseline of the Age-Well randomized controlled trial (RCT) of the Medit-Ageing European Project, sponsored by the French National Institute of Health and Medical Research (Inserm) [34]. Data were acquired between 2016 and 2020. All participants were community-dwelling individuals aged over 65 years old, and performed in the normal range for their age and education level on standardized cognitive tests of a neuropsychological diagnostic battery. Those with contraindications in relation to MRI or PET scanning, evidence of a major neurological or psychiatric disorder (including alcohol or drug abuse), history of cerebrovascular disease, presence of a chronic disease or acute unstable illness, and current or recent medication that may interfere with cognitive functioning were not included. At baseline, they underwent a comprehensive neuropsychological assessment, an ambulatory polysomnography (PSG) recording, structural MRI and <sup>18</sup>F-Florbetapir PET scans and Apolipoprotein E (ApoE) genotyping within a maximum interval of 3 months. Then, they were randomly assigned to one of the 3 arms of an 18-month intervention (meditation training, non-native language training or no intervention group). At follow-up, they repeated structural MRI and <sup>18</sup>F-Florbetapir PET examinations (see below). All participants gave their written informed consent prior to the examinations, and the Age-Well RCT was approved by the ethics committee (CPP Nord-Ouest III, Caen; trial registration number: EudraCT: 2016-002441-36; IDRCB: 2016-A01767-44; ClinicalTrials.gov Identifier: NCT02977819).

### Polysomnography recording

Participants underwent an ambulatory PSG recording at home using a Siesta® device (Compumedics, Australia). Eighty-one participants over 121 (67% of the sample) had a habituation night at the beginning of the protocol, which was not included in the analyses. The PSG consisted in recording the electroencephalogram (EEG), electrooculogram (EOG), electrocardiogram (ECG), chin

electromyogram (EMG), respiratory movements using thoracic and abdominal belts, respiratory airflow using nasal and oral thermistors, and oxygen saturation using a finger pulse oximeter. For the EEG recording, we placed 20 electrodes over the scalp according to the international 10-20 system (Fp1, Fp2, F3, F4, F7, F8, Fz, C3, C4, Cz, T3, T4, P3, P4, Pz, O1, O2, vertex ground, and a bi-mastoid reference), with impedances kept below 5 k $\Omega$ . The EEG signal was digitalized at a sampling rate of 256 Hz, high-pass and low-pass filters were applied, respectively at 0.3 Hz, and 35 Hz. Recordings were visually scored in 30-second epochs according to the rules of the American Academy of Sleep Medicine [35], allowing the computation of standard sleep parameters and respiratory parameters used as covariates in the analyses, including the apnea-hypopnea index (AHI, sum of apneas and hypopneas per hour of sleep), the proportion of total sleep time with SpO<sub>2</sub> level  $\leq$  90% and the density of respiratory micro-arousals (number of events per hour of sleep).

### Spectral analyses

Spectral analyses were performed on all artefact-free N2 and N3 sleep epochs using Matlab R2018b (Mathworks, Natick, USA) and the free open-source toolbox Sleeptrip (<https://github.com/Frederik-D-Weber/sleeptrip>; RRID: SCR\_017318) based on FieldTrip functions (<http://fieldtriptoolbox.org>; RRID: SCR\_004849) [36]. An independent component analysis (ICA) was carried out for 2 subjects to remove ECG artefacts on EEG data, and the resulting EEG signals were visually inspected for quality check purposes. Data were then epoched into 5-s bins and those containing manually identified EEG artefacts or movement arousals were rejected. Channels with artefacts affecting a majority of the recording were also removed. Power spectral analyses were performed on continuous 4-s segments (50% overlap) and were tapered using a Hanning window. A fast Fourier Transform was applied. The power spectra were averaged across all segments (Welch's method) and normalized by the effective noise bandwidth to obtain power spectral density estimates for the whole data (spectral resolution of 0.25 Hz). For each electrode, mean power was calculated in delta (0.5-4 Hz) frequency band, normalized by total power to account for potential individual differences in absolute spectral power.

As in previous studies, we separated slow (0.5-1 Hz) and fast (1-4 Hz) delta sub-bands using a cut-off of 1Hz [29–31,33]. A ratio between slow and fast delta power was also computed. To reduce the number of analyses and obtain topographically-specific values, spectral power was averaged on several channels as follows: frontal (F3, Fz, F4), central (C3, Cz, C4), parietal (P3, Pz, P4), temporal (T3, T4), and occipital (O1, O2). As delta power is particularly reduced in frontal areas with age, we focused the main analyses on frontal delta power, and other regions were used for replication purposes. Consistently with recent recommendations for sleep research in older adults [37], spectral power was computed on N2 and N3 sleep epochs (referred to as N2-N3 sleep hereafter), but sensitivity analyses were also performed using N3 epochs only. Finally, as delta power is known to decay across sleep cycles during the night, spectral analyses were also performed during the N2-N3 epochs of the first and second half of night separately (the cut-off point being defined as the epoch equally distant from the first and last epochs of sleep).

## Neuroimaging examinations

All neuroimaging examinations were performed at the Cyceron Center (Caen, France) on the same MRI and PET cameras (Philips Achieva 3T and a GE Healthcare Discovery RX VCT 64 PET-CT scanners, respectively).

### 1) Structural MRI

High-resolution T1-weighted anatomical images were acquired at baseline and follow-up using a 3D fast-field echo sequence (3D-T1-FFE sagittal, repetition time = 7.1 ms, echo time = 3.3 ms, flip angle = 6°, 180 slices with no gap, slice thickness = 1 mm, field of view = 256 x 256 mm<sup>2</sup>, in-plane resolution = 1 x 1 x 1 mm<sup>3</sup>). During the MRI sessions, subjects were equipped with earplugs and their head was stabilized with foam pads to minimize head motion. T1-weighted images were segmented using FLAIR images (3D-IR sagittal, TR/TE/TI = 4800/272/1650 ms ; flip angle = 40°; 180 slices with no gap; slice thickness = 1 mm; field of view = 250 x 250 mm<sup>2</sup>; in-plane resolution = 0.98 x 0.98 mm<sup>2</sup>), spatially normalized to the Montreal Neurological Institute (MNI) template, modulated using the

SPM12 segmentation procedure (<http://www.fil.ion.ucl.ac.uk>) and smoothed with an 8 mm full-width at half-maximum (FWHM) Gaussian filter. Images were then masked to exclude non-gray matter voxels from the analyses.

## 2) PET imaging

Florbetapir-PET scans were performed at baseline and follow-up to reflect both brain perfusion (early acquisition) and amyloid deposition (late acquisition). They were acquired with a resolution of  $3.76 \times 3.76 \times 4.9 \text{ mm}^3$  (field of view = 157 mm). Forty-seven planes were obtained with a voxel size of  $1.95 \times 1.95 \times 3.27 \text{ mm}^3$ . A transmission scan was performed for attenuation correction before the PET acquisition. Each participant underwent a 10 min PET scan beginning at the intravenous injection of  $\sim 4 \text{ MBq/Kg}$  of Florbetapir, and another 10 min scan beginning 50 min after the injection. Due to an injection issue, early and late PET data at baseline were missing for one participant, and late PET data at baseline were not available for one participant due to acquisition issues.

Early Florbetapir-PET was reconstructed from 1 to 5 min. PET images were coregistered on their corresponding anatomical MRI and were then normalized to the MNI template using deformation parameters derived from the anatomical MRI. Resulting images were scaled using cerebellar GM as a reference. A smoothing kernel of 10 mm Gaussian filter was applied and images were masked to exclude non-gray matter voxels from the analyses. To determine participants' amyloid positivity, individual global cortical amyloid standardized uptake value ratio (SUVR) was extracted from a predetermined neocortical mask (including the entire GM, except the cerebellum, occipital and sensory motor cortices, hippocampi, amygdala and basal nuclei) [38]. A similar procedure with white matter scaling was also applied on baseline and follow-up images to specifically assess global amyloid accumulation over time (estimated with difference between follow-up and baseline SUVR) as this procedure is more sensitive to estimate SUVR longitudinal changes [39,40].

Maps reflecting amyloid percent annual changes (i.e., PET-PAC maps) between baseline and follow-up were generated for each participant. To do so, a customized DARTEL (Diffeomorphic Anatomical Registration through Exponentiated Lie Algebra) template was obtained from baseline MRI scans. For

each participant, a pairwise longitudinal registration was computed between baseline and follow-up anatomical MRI images, resulting in a midpoint average anatomical MRI image (i.e., anatomical MRI average). The anatomical MRI average was segmented into GM, white matter and CSF, and was then normalized to the DARTEL template. Baseline and follow-up late Florbetapir-PET images were 1) coregistered on the anatomical MRI average, 2) normalized to the DARTEL template by applying the deformation parameters from the corresponding anatomical MRI average, and 3) scaled by white matter. The resulting PET images were used to create individual PET-PAC maps. PET-PAC maps represent the voxel-wise calculation of percent amyloid change over the follow-up period (i.e. the difference between follow-up and baseline scaled PET value divided by baseline PET value x 100) expressed in annual percent change (i.e. multiplied by 12/number of months between baseline and follow-up PET scans). This calculation was performed only on voxels common to both baseline and follow-up PET data, identified using a masking procedure. A differential smoothing ( $8.1 \times 8.1 \times 7.5 \text{ mm}^3$ ) was then applied to the PET-PAC maps.

### Statistical analyses

First, we aimed at assessing the neural correlates of N2-N3 sleep delta power in the different frequency ranges (i.e., delta, slow and fast delta) at baseline. Thus, voxel-wise multiple regressions were performed between natural log values of frontal delta power during N2-N3 sleep and GM volume, brain perfusion and amyloid burden at baseline, separately. Regressions between neuroimaging data and the ratio between slow and fast delta power were also carried out. All analyses were controlled for age, sex, education, ApoE4 status and the AHI.

Second, we investigated whether baseline delta power in the different frequency ranges was associated with longitudinal amyloid changes. Therefore, similar voxel-wise multiple regressions were performed between log values of delta power and PET-PAC maps masked to keep only the voxels accumulating amyloid. This mask was composed of all significant positive voxels ( $p < 0.005$ ,

uncorrected) in a one-sample t test performed on PET-PAC maps. The same covariates were added in the model (i.e., age, sex, education, AHI and ApoE4 status), with the addition of the intervention group (i.e., passive control, non-native foreign language training and meditation training, coded categorically), as assessing the impact of non-pharmacological interventions on sleep was not the aim of the present study.

Then, sensitivity and specificity analyses were performed to ensure of the robustness of the results. We aimed at replicating all main results with (i) N2-N3 sleep delta power values computed on other EEG derivations (i.e., central, parietal, temporal and occipital channels), (ii) frontal delta power computed on N3 sleep epochs only, and (iii) by adding the presence of the habituation night (coded as 0 or 1) as a covariate, to ensure that the absence of a habituation night had no impact. Furthermore, we checked whether our main results were replicated when computing spectral power during N2-N3 epochs of the first *versus* second half of the night, to account for the dynamic of delta power (and its sub-bands) across sleep cycles. Finally, as the AHI was relatively high in our cohort, we performed a series of confirmatory analyses to ensure that this did not impact our results. The characteristics of individuals with and without severe sleep apnea were compared using t tests for continuous variables and Chi<sup>2</sup> for categorical variables (**Supplementary Table 1**). First, we replicated the analyses in a subsample excluding participants with severe sleep apnea, as measured by an AHI  $\geq$  30. Second, we repeated the main analyses by controlling for hypoxemia and sleep fragmentation-related variables (i.e., proportion of total sleep time with SpO2 level  $\leq$  90% and density of respiratory micro-arousals) instead of the AHI alone.

All neuroimaging analyses were carried out using SPM12, and results were considered significant at a  $p < 0.005$  (uncorrected) threshold combined with an analysis-specific minimum cluster size (**Supplementary Table 2**) determined by Monte-Carlo simulations using the AlphaSim program to achieve a corrected statistical significance of  $p < 0.05$ .

## Results

### Participants characteristics

The flowchart of the inclusion process is available in **Figure 1** and participants' characteristics are summarized in **Table 1**. From the 137 participants enrolled in the Age-Well RCT, 127 were included in baseline cross-sectional analyses, and 113 in longitudinal analyses after a mean follow-up of  $20.7 \pm 0.9$  months (**Figure 1**). At baseline, participants had a mean age of  $69.0 \pm 3.8$  years, 63% of the sample were women and 20.6% were amyloid-positive. The distribution of sleep-disordered breathing severity among the cohort was as follow:  $AHI < 15$  ( $n=32$ ),  $15 \leq AHI < 30$  ( $n=59$ ),  $AHI \geq 30$  ( $n=36$ ). The mean  $\Delta$  SUVR value, reflecting amyloid accumulation over the follow-up period, was  $0.0039 \pm 0.027$  (see the distribution in **Figure 2**). Of note, only 16 of 113 participants (14% of the cohort) had an increase of at least 5% of the SUVR over the follow-up period, and only 2 (1.8% of the cohort) had an increase of at least 10%.

Specificity analyses were carried out in participants without severe sleep apnea (i.e., with  $AHI < 30$ ). This group differed from participants with severe sleep apnea (i.e., with  $AHI \geq 30$ ) only in terms of sex-ratio ( $p = 0.035$ ), which was controlled for in statistical analyses (**Supplementary Table 1**).

### N2-N3 sleep delta power, GM volume and brain perfusion at baseline

#### 1) GM volume

We first assessed voxel-wise associations between frontal delta power and GM volume. Higher delta (0.5-4 Hz) power during N2-N3 sleep was associated with higher GM volume mainly in the medial orbitofrontal cortex (mOFC), bilateral middle frontal gyrus, anterior and middle cingulate gyri, extending to some temporal and posterior cortical areas (e.g., fusiform, lingual, middle and inferior temporal gyri) (**Figure 3A, Table 2**). Furthermore, higher slow delta (0.5-1 Hz) power was associated with higher GM volume mainly in the mOFC and anterior cingulate cortex (ACC) (**Figure 3B, Table 2**).

Interestingly, an opposite association was found with fast delta (1-4 Hz), such that higher fast delta power was associated with atrophy in the mOFC and bilateral ACC (**Figure 3C, Table 2**). Consistently, lower GM volume in the mOFC and bilateral ACC was also associated with lower ratio between slow and fast delta power (**Figure 3D, Table 2**). Finally, a positive correlation was also found between fast delta power and GM volume in the left temporal middle gyrus (**Table 2**).

Results were replicated when calculating delta power over central, parietal, temporal or occipital channels, except for fast delta, for which only the positive associations with central and temporal channels survived the cluster size correction (**Supplementary Figure 1**). In addition, the same pattern of results was obtained when (i) computing delta power only in N3 epochs (**Supplementary Figure 2, Supplementary Table 3**), (ii) excluding participants with severe sleep apnea (**Supplementary Figure 3A**), (iii) adding the presence or not of a habituation night as a covariate and (iv) taking into account hypoxemia and sleep fragmentation.

Interestingly, all main associations between spectral power values and fronto-cingulate GM volume were replicated when computing spectral power values during N2-N3 epochs of the first or the second half of the night (**Supplementary Figure 4**).

## 2) Brain perfusion

We then investigated voxel-wise associations between frontal delta power and brain perfusion. No significant association was found between frontal delta power and brain perfusion (**Figure 3A**). However, secondary analyses revealed that parietal and occipital delta power were positively associated with perfusion in the right middle frontal gyrus (**Supplementary Figure 5**).

When considering delta sub-bands, positive associations were observed between perfusion in the mOFC and ACC and slow delta power (0.5-1 Hz) on all derivations (see **Table 2** and **Figure 3B** for frontal derivations, and **Supplementary Figure 5** for other derivations), such that higher perfusion in these regions was related to higher slow delta power. No significant association was found between fast delta (1-4 Hz) power and brain perfusion (**Figure 3C**). However, a lower ratio between slow and

fast delta power was associated with lower brain perfusion in the mOFC and bilateral ACC (**Figure 3D, Table 2**).

Sensitivity and specificity analyses revealed that all results were similar after taking into account hypoxemia and sleep fragmentation. Similarly, the pattern of results was confirmed when computing delta power on N3 epochs only, except that the cluster associated with the slow/fast ratio did not survive the cluster size correction (**Supplementary Figure 2, Supplementary Table 3**). Likewise, results with slow delta were replicated in the subgroup excluding participants with severe sleep apnea, and the clusters with the other frequency bands were present but did not survive the cluster size correction (**Supplementary Figure 3B**). Lastly, adding the habituation night as a covariate yielded similar results, except for the analysis with fast delta power during N2-N3 sleep in the entire cohort that revealed a significant cluster in the mOFC and bilateral ACC (cluster size: 3021 mm<sup>3</sup>, t-value = 3.42). Of note, results remained unchanged when computing spectral power values on the first or the second half of the night, except that the frontal cluster associated with slow/fast ratio on the first half of the night did not survive the cluster size correction (**Supplementary Figure 4**).

### N2-N3 sleep delta power, amyloid burden and accumulation over time

At baseline, neither delta, slow, fast delta power, nor the slow/fast ratio during N2-N3 or N3 sleep were associated with amyloid burden. This absence of association was observed for all EEG derivations, when excluding participants without severe sleep apnea (**Supplementary Figure 3C**), and when taking into account the presence of a habituation night or hypoxemia and sleep fragmentation in the models.

Regarding longitudinal analyses, amyloid PAC was neither associated with delta power in the different sub-bands, nor with the ratio of slow over fast delta power, during N2-N3 or N3 sleep. Again, similar results were obtained regardless of the EEG derivations, when considering only participants without severe sleep apnea (**Supplementary Figure 3D**), and when taking into account the presence of a habituation night or hypoxemia and sleep fragmentation in the models.

Finally, amyloid burden at baseline and amyloid PAC were not associated with spectral power values computed on N2-N3 epochs of the first and the second half of the night (**Supplementary Figure 4**).

## Discussion

Our main objective was to investigate the neural correlates of N2-N3 delta power sub-bands in cognitively unimpaired older adults, using multimodal neuroimaging. Our results reveal opposite associations between delta power sub-bands and brain integrity, with higher slow delta power being associated with higher mOFC and ACC volume and perfusion, while higher fast delta power is related to lower volume and perfusion in these regions. In contrast, no significant association was found with amyloid deposition, even when considering delta power sub-bands or their ratio.

Slow waves, which mainly contribute to delta power, are known to originate from medial prefrontal and anterior cingulate areas [41], and to propagate along an antero-posterior axis [42]. They play a key role in memory consolidation [43] and in the clearance of cerebral toxic waste such as A $\beta$  [27]. Delta power decreases with age [2,10,11,13,16] and this reduction has been associated with impaired sleep-dependent memory consolidation [12,14] and a greater risk of cognitive impairment [44]. Here, our results support previous studies showing that brain atrophy in regions involved in the generation and propagation of slow waves (e.g., fronto-cingulate regions) likely underlies the age-related decrease in delta power in older adults [14–16]. We also observed an association with brain perfusion, which was probably weaker as it was restricted to the right cerebral hemisphere and for parietal and occipital channels only, while similar clusters in the left hemisphere were present but under the corrected threshold. Some authors suggest that delta power in the slow *versus* fast sub-bands may have different physiological properties and play distinct roles [45]. For instance, only delta power above 2 Hz usually declines from the first to the second NREM sleep episode of a given night [46]. Furthermore, only the fast component of delta power increases after sleep deprivation in both mice [47] and humans [48]. To our knowledge, we report for the first time in humans that the

links between delta power and frontal GM volume and perfusion vary according to the frequency bands considered. Indeed, higher slow delta power (0.5-1 Hz) was associated with higher mOFC and ACC volume and perfusion, while an opposite pattern, at least with GM volume, was found with fast delta power (1-4 Hz). These findings were replicated when analyzing the first and the second half of the night separately and suggest that the slower component of delta power is the largest contributor of the likely bidirectional positive associations between delta power and GM volume [12,14,16] and metabolism [17] previously reported in the literature. Consistently, a higher ratio between slow and fast delta power was also associated to higher GM volume and perfusion in the mOFC and ACC. Age-related structural and/or functional changes in these areas may particularly affect the ability of the brain to generate the slowest EEG rhythms during NREM sleep, leading to a shift towards faster delta frequencies and an increase of the relative contribution of fast delta power. Of note, we also reported an association between higher fast delta power and greater GM volume in the left temporal middle gyrus. This association was marginal, considering that no other frequency band and neuroimaging modality (e.g., perfusion) correlated with this cluster. Further studies are needed to test the robustness of this association.

We did not observe any significant association between delta sub-band powers and amyloid deposition. This result stands at odds with some previous studies showing opposite relationships between slow and fast delta powers and amyloid pathology, with greater slow delta power being associated with less amyloid burden [29,30,32] and accumulation over time [31], while higher fast delta power was related to greater A $\beta$  burden [29] and accumulation over time [31]. In addition, it has also been shown that inducing faster delta power for 1 month using optogenetics exacerbates amyloid peptide accumulation in a transgenic mice model of Alzheimer's disease [49]. In our sample, we did not replicate previous findings showing that slow delta power is negatively associated with amyloid burden [29,30,32], even when considering specifically delta power during N3 sleep. While animal studies support robust associations between reduced delta power and greater amyloid deposition [50], clinical studies assessing the links between sleep disturbances, including altered N3,

and amyloid levels measured using PET-imaging are more heterogeneous. Indeed, a substantial part of studies reporting significant associations between sleep and PET-measured amyloid burden have used self-reported sleep measures [51–55], and have not always been replicated, even in large cohorts [56,57]. Importantly, self-reported sleep parameters are known to frequently differ from objective sleep measures, especially in older populations [58–60]. When considering objectively-measured sleep, the links between N3 and amyloid levels have mainly been demonstrated using CSF measures [26–28,61]. Amyloid burden measured using PET (that reflects the accumulation of the amyloid peptide over a longer period) has been previously associated with several sleep parameters derived from polysomnography including slow delta power [29,30,32], the coupling between sleep spindles and a subtype of slow waves [33] and specific subtypes of sleep arousals (depending on their propensity to trigger sleep stage transition and the concomitant EMG activity) [62]. Of note, studies reporting associations with slow delta power are heterogeneous in terms of the frequency band considered (0.6-1 Hz [29,30] or 1-2 Hz [32]), have relatively limited sample size (< 40 participants), often include highly educated individuals (16 to 17 years of education on average [29,30]) and partially overlapping cohorts [29–31]. Importantly, a recent study with a large, yet younger sample (n = 100 individuals aged between 50 and 70 years) did not report significant associations between delta sub-band powers and amyloid burden [33]. Similarly, we did not find any association between PET-measured amyloid burden and delta power or its sub-bands in N3 and N2-N3 sleep, despite a sample size from 3 to 4 times larger than in studies reporting significant results. Several factors may explain these discrepancies in clinical studies, with the main difference across cohorts being the proportion of amyloid positive participants. Indeed, 21% of the participants in our cohort were amyloid-positive, which is substantially lower compared to previous studies (45% in [32] and 61% in [30]). Thus, cohorts with younger participants [33] and/or a lower proportion of amyloid-positive participants may not have sufficient variability to reveal significant associations between amyloid burden and delta power. Similarly, the absence of association between delta sub-band powers and amyloid accumulation over time in our cohort is likely due to the fact that our

participants exhibited very modest changes in amyloid load over the relatively short 21-month follow-up, compared to the 3.7 years follow-up in the only study testing the associations with longitudinal amyloid changes [31]. Further longitudinal studies following individuals with higher amyloid load over several years are needed to clarify the complex relationship between delta power and amyloid pathology. The inclusion/exclusion of participants with sleep-disordered breathing may represent another important factor explaining discordant results, as it has been associated with greater amyloid burden and changes in GM volume, perfusion and metabolism [63,64]. Previous studies investigating the associations between delta sub-bands and amyloid have excluded participants with an AHI  $\geq 15$  [29,31,33], or included a smaller proportion of individuals with sleep-disordered breathing (13% [32]) than in our sample. As sleep-disordered breathing is highly prevalent and underdiagnosed in older individuals, our cohort may be more representative of the general older population [65,66]. If in our cohort there was a high proportion of individuals with an AHI  $\geq 15$  (n=95 individuals; 75% of the sample), these participants were overall poorly symptomatic, with only 15 presenting an Epworth Sleepiness Scale score  $\geq 9$ , suggestive of excessive daytime sleepiness. In addition, we replicated our results after controlling for the AHI or its related effects on oxygen saturation and sleep fragmentation, and after excluding participants with severe sleep apnea. We therefore believe that sleep-disordered breathing had no major impact on our results, which aligns with another study showing no link between amyloid pathology and delta sub-band power, which excluded individuals with AHI  $\geq 15$  [33]. It is possible that differences in lifestyle (e.g., practice of physical and/or cognitive activities) and psycho-affective factors between cohorts may explain part of the observed differences.

### Strengths and limitations

Our study has several strengths, including the computation of delta power across several frequency sub-bands in both N2-N3 and N3 sleep to finely investigate its neural correlates. In addition, we

combined four complementary neuroimaging measures (GM volume, brain perfusion, amyloid burden and its accumulation over time) in a relatively large sample of cognitively unimpaired individuals. Analyses were controlled for important confounders, including the ApoE4 status, sleep apnea and its related effects on oxygen saturation and sleep fragmentation. Sensitivity analyses were also performed in a subgroup of participants to rule out the possible influence of severe sleep apnea. The temporal dynamic of delta power across the night has also been considered by replicating the results in NREM epochs of the first and second half of the night separately, even if the dynamic for each sleep cycle has not been specifically addressed. However, this study also has limitations. First, all participants did not have a habituation night, but we replicated our findings after controlling for this variable. Second, the relatively low amyloid burden at baseline and accumulation over time is likely to explain the absence of association between delta power and amyloid deposition and accumulation. Future studies will need to use longer longitudinal designs in more diverse samples to investigate the relationships between spectral power in delta sub-bands and the accumulation of amyloid over time.

## Conclusion

Overall, our results demonstrate that the known links between reduced NREM sleep delta power and altered brain integrity in fronto-cingulate regions are mainly driven by the EEG power below 1 Hz. Moreover, slow (0.5-1 Hz) and fast (1-4 Hz) delta power show opposite associations with fronto-cingulate GM volume and perfusion. Importantly, these associations appear to be more specific than when using the entire delta frequency band. In addition, we found no significant associations between delta power and amyloid burden, regardless of the frequency band used. Further studies investigating the links between NREM sleep delta power and brain and cognitive integrity should consider analysing slow and fast delta power separately.

## Acknowledgements

The authors would like to thank the participants of the study for their contribution, as well as Franck Doidy, Sébastien Polvent and Dr Alison Mary for their help with polysomnography acquisition and scoring. We are grateful to the Cyceron MRI-PET staff for their help with recruitment and neuroimaging data acquisition, and to Aurélia Cognet, Valérie Lefranc and Géraldine Poinsel for their administrative support. We acknowledge the contribution of all members of the Medit-Ageing Research Group (Alexandre Bejanin<sup>1</sup>, Léa Chauveau<sup>1</sup>, Anne Chocat<sup>1</sup>, Fabienne Collette<sup>2,3,4</sup>, Sophie Dautricourt<sup>1</sup>, Robin De Flores<sup>1</sup>, Marion Delarue<sup>1</sup>, Harriet Demnitz-King<sup>5</sup>, Hélène Espérou<sup>6</sup>, Séverine Fauvel<sup>1</sup>, Francesca Felisatti<sup>1</sup>, Eglantine Ferrand Devouge<sup>1,7,8</sup>, Eric Frison<sup>9,10</sup>, Julie Gonneaud<sup>1</sup>, Sacha Haudry<sup>1</sup>, Oriane Hébert<sup>1</sup>, Olga Klimecki<sup>11,12</sup>, Elizabeth Kuhn<sup>1</sup>, Brigitte Landeau<sup>1</sup>, Valérie Lefranc<sup>1</sup>, Natalie Marchant<sup>5</sup>, Florence Mezenge<sup>1</sup>, Cassandre Palix<sup>1</sup>, Anne Quillard<sup>1</sup>, Florence Requier<sup>2</sup>, Eric Salmon<sup>13</sup>, Edelweiss Tournon<sup>1</sup>, Anne-Laure Turpin<sup>1</sup>, Patrik Vuilleumier<sup>14</sup>, Tim Whitfield<sup>5</sup>, Miranka Wirth<sup>15,16</sup>).

<sup>1</sup> Normandie Univ, UNICAEN, INSERM, U1237, PhIND Physiopathology and Imaging of Neurological Disorders, Institut Blood and Brain @ Caen-Normandie, Cyceron, 14000 Caen, France.

<sup>2</sup> GIGA-CRC In Vivo Imaging, Université de Liège, National Fund for Scientific Research (F.R.S-FNRS), Liège, Belgium.

<sup>3</sup> Psychology and Neuroscience of Cognition, University of Liège, Liège, Belgium.

<sup>4</sup> Fund for Scientific Research FNRS, 1000, Brussels, Belgium.

<sup>5</sup> Division of Psychiatry, University College London, London, United Kingdom.

<sup>6</sup> Inserm, pôle de recherche clinique, institut de santé publique, 75013 Paris, France.

<sup>7</sup> Normandie Univ, UNIROUEN, Department of General Practice, Rouen, France.

<sup>8</sup> Rouen University Hospital, CIC-CRB 1404, F 76000, Rouen, France.

<sup>9</sup> EUCLID/F-CRIN Clinical Trials Platform, Univ. Bordeaux, Inserm, Bordeaux Population Health Center, Bordeaux, France.

<sup>10</sup> CHU Bordeaux, Service d'information médicale, Bordeaux, France.

<sup>11</sup> Swiss Center for Affective Sciences, Department of Medicine and Department of Psychology, University of Geneva, Geneva, Switzerland.

<sup>12</sup> Clinical Psychology and Behavioral Neuroscience, Faculty of Psychology, Technische Universität Dresden, 01187, Dresden, Germany.

<sup>13</sup> Division of Nuclear Medicine, Department of Medical Physics, Cyclotron Research Center, University Hospital of Liège, University of Liège, Liège, Belgium.

<sup>14</sup> Swiss Center for Affective Sciences, University of Geneva, Geneva, Switzerland; Laboratory for Behavioral Neurology and Imaging of Cognition, Department of Neuroscience, Medical School, University of Geneva, Geneva, Switzerland.

<sup>15</sup> Charité-Universitätsmedizin Berlin, corporate member of Freie Universität Berlin, Humboldt-Universität zu Berlin and Berlin Institute of Health, NeuroCure Clinical Research Center, Berlin, Germany.

<sup>16</sup> German Center for Neurodegenerative Diseases (DZNE), Dresden, Germany.

The Age-Well RCT is part of the Medit-Ageing project funded through the European Union's Horizon 2020 research and innovation program (grant agreement n° 667696), Inserm, Region Normandie, and Fondation d'entreprise MMA des Entrepreneurs du Futur. PC was funded by a PhD grant (Contrat Doctoral Spécifique Normalien). CA was funded by INSERM, Région Normandie and the Fonds Européen de Développement Régional (FEDER). Complementary funding sources were obtained from Association France Alzheimer (grant n° 1714), Fondation LECMA-Vaincre Alzheimer (grant n° 13732) and Fondation Thérèse et René Planiol. Funding sources were not involved in the study design, data acquisition, analysis, interpretation or manuscript writing.

## Disclosure Statement

Financial Disclosure: none.

Non-financial Disclosure: none.

## References

1. Mander BA, Winer JR, Walker MP. Sleep and Human Aging. *Neuron*. 2017;94(1):19-36. doi:10.1016/j.neuron.2017.02.004
2. Carrier J, Land S, Buysse DJ, Kupfer DJ, Monk TH. The effects of age and gender on sleep EEG power spectral density in the middle years of life (ages 20-60 years old). *Psychophysiology*. 2001;38(2):232-242. doi:10.1111/1469-8986.3820232
3. Ohayon MM, Carskadon MA, Guilleminault C, Vitiello MV. Meta-Analysis of Quantitative Sleep Parameters From Childhood to Old Age in Healthy Individuals: Developing Normative Sleep Values Across the Human Lifespan. *Sleep*. 2004;27(7):1255-1273. doi:10.1093/sleep/27.7.1255
4. Petit D, Gagnon JF, Fantini ML, Ferini-Strambi L, Montplaisir J. Sleep and quantitative EEG in neurodegenerative disorders. *Journal of Psychosomatic Research*. 2004;56(5):487-496. doi:10.1016/j.jpsychores.2004.02.001
5. Vyazovskiy VV, Riedner BA, Cirelli C, Tononi G. Sleep Homeostasis and Cortical Synchronization: II. A Local Field Potential Study of Sleep Slow Waves in the Rat. *Sleep*. 2007;30(12):1631-1642. doi:10.1093/sleep/30.12.1631
6. Neckelmann D, Ursin R. Sleep Stages and EEG Power Spectrum in Relation to Acoustical Stimulus Arousal Threshold in the Rat. *Sleep*. 1993;16(5):467-477. doi:10.1093/sleep/16.5.467
7. Kurth S, Ringli M, LeBourgeois MK, et al. Mapping the electrophysiological marker of sleep depth reveals skill maturation in children and adolescents. *NeuroImage*. 2012;63(2):959-965. doi:10.1016/j.neuroimage.2012.03.053
8. Asyali MH, Berry RB, Khoo MCK, Altinok A. Determining a continuous marker for sleep depth. *Computers in Biology and Medicine*. 2007;37(11):1600-1609. doi:10.1016/j.compbiomed.2007.03.001
9. Younes M, Schweitzer PK, Griffin KS, Balshaw R, Walsh JK. Comparing two measures of sleep depth/intensity. *Sleep*. 2020;43(12):zsaa127. doi:10.1093/sleep/zsaa127
10. Landolt HP, Dijk DJ, Achermann P, Borbély AA. Effect of age on the sleep EEG: slow-wave activity and spindle frequency activity in young and middle-aged men. *Brain Research*. 1996;738(2):205-212. doi:10.1016/S0006-8993(96)00770-6
11. Landolt HP, Borbély AA. Age-dependent changes in sleep EEG topography. *Clinical Neurophysiology*. 2001;112(2):369-377. doi:10.1016/S1388-2457(00)00542-3
12. Varga AW, Ducca EL, Kishi A, et al. Effects of aging on slow-wave sleep dynamics and human spatial navigational memory consolidation. *Neurobiology of Aging*. 2016;42:142-149. doi:10.1016/j.neurobiolaging.2016.03.008

13. Gao C, Scullin MK. Longitudinal trajectories of spectral power during sleep in middle-aged and older adults. *Aging Brain*. 2023;3:100058. doi:10.1016/j.nbas.2022.100058
14. Mander BA, Rao V, Lu B, et al. Prefrontal atrophy, disrupted NREM slow waves and impaired hippocampal-dependent memory in aging. *Nat Neurosci*. 2013;16(3):357-364. doi:10.1038/nn.3324
15. Dube J, Lafortune M, Bedetti C, et al. Cortical Thinning Explains Changes in Sleep Slow Waves during Adulthood. *Journal of Neuroscience*. 2015;35(20):7795-7807. doi:10.1523/JNEUROSCI.3956-14.2015
16. Latreille V, Gaubert M, Dubé J, Lina JM, Gagnon JF, Carrier J. Age-related cortical signatures of human sleep electroencephalography. *Neurobiology of Aging*. 2019;76:106-114. doi:10.1016/j.neurobiolaging.2018.12.012
17. Wilckens KA, Aizenstein HJ, Nofzinger EA, et al. The role of non-rapid eye movement slow-wave activity in prefrontal metabolism across young and middle-aged adults. *Journal of Sleep Research*. 2016;25(3):296-306. doi:10.1111/jsr.12365
18. Ju YES, Lucey BP, Holtzman DM. Sleep and Alzheimer disease pathology—a bidirectional relationship. *Nat Rev Neurol*. 2014;10(2):115-119. doi:10.1038/nrneurol.2013.269
19. André C, Laniepe A, Chételat G, Rauchs G. Brain changes associated with sleep disruption in cognitively unimpaired older adults: A short review of neuroimaging studies. *Ageing Research Reviews*. 2021;66:101252. doi:10.1016/j.arr.2020.101252
20. Kang JE, Lim MM, Bateman RJ, et al. Amyloid- $\beta$  Dynamics are Regulated by Orexin and the Sleep-Wake Cycle. *Science*. 2009;326(5955):1005-1007. doi:10.1126/science.1180962
21. Roh JH, Huang Y, Bero AW, et al. Disruption of the Sleep-Wake Cycle and Diurnal Fluctuation of  $\beta$ -Amyloid in Mice with Alzheimer's Disease Pathology. *Science Translational Medicine*. 2012;4(150):150ra122-150ra122. doi:10.1126/scitranslmed.3004291
22. Huang Y, Potter R, Sigurdson W, et al. Effects of Age and Amyloid Deposition on A $\beta$  Dynamics in the Human Central Nervous System. *Archives of Neurology*. 2012;69(1):51-58. doi:10.1001/archneurol.2011.235
23. Xie L, Kang H, Xu Q, et al. Sleep Drives Metabolite Clearance from the Adult Brain. *Science*. 2013;342(6156):373-377. doi:10.1126/science.1241224
24. Hablitz LM, Vinitsky HS, Sun Q, et al. Increased glymphatic influx is correlated with high EEG delta power and low heart rate in mice under anesthesia. *Science Advances*. 2019;5(2):eaav5447. doi:10.1126/sciadv.aav5447

25. Fultz NE, Bonmassar G, Setsompop K, et al. Coupled electrophysiological, hemodynamic, and cerebrospinal fluid oscillations in human sleep. *Science*. 2019;366(6465):628-631. doi:10.1126/science.aax5440
26. Varga AW, Wohlleber ME, Giménez S, et al. Reduced Slow-Wave Sleep Is Associated with High Cerebrospinal Fluid A $\beta$ 42 Levels in Cognitively Normal Elderly. *Sleep*. 2016;39(11):2041-2048. doi:10.5665/sleep.6240
27. Ju YES, Ooms SJ, Sutphen C, et al. Slow wave sleep disruption increases cerebrospinal fluid amyloid- $\beta$  levels. *Brain*. 2017;140(8):2104-2111. doi:10.1093/brain/awx148
28. Ju YES, Zangrilli MA, Finn MB, Fagan AM, Holtzman DM. Obstructive sleep apnea treatment, slow wave activity, and amyloid- $\beta$ . *Annals of Neurology*. 2019;85(2):291-295. doi:10.1002/ana.25408
29. Mander BA, Marks SM, Vogel JW, et al.  $\beta$ -amyloid disrupts human NREM slow waves and related hippocampus-dependent memory consolidation. *Nature Neuroscience*. 2015;18(7):1051-1057. doi:10.1038/nn.4035
30. Winer JR, Mander BA, Helfrich RF, et al. Sleep as a Potential Biomarker of Tau and  $\beta$ -Amyloid Burden in the Human Brain. *J Neurosci*. 2019;39(32):6315-6324. doi:10.1523/JNEUROSCI.0503-19.2019
31. Winer JR, Mander BA, Kumar S, et al. Sleep Disturbance Forecasts  $\beta$ -Amyloid Accumulation across Subsequent Years. *Current Biology*. 2020;30(21):4291-4298.e3. doi:10.1016/j.cub.2020.08.017
32. Lucey BP, McCullough A, Landsness EC, et al. Reduced non-rapid eye movement sleep is associated with tau pathology in early Alzheimer's disease. *Science Translational Medicine*. 2019;11(474):eaau6550. doi:10.1126/scitranslmed.aau6550
33. Chylinski D, Van Egroo M, Narbutas J, et al. Timely coupling of sleep spindles and slow waves linked to early amyloid- $\beta$  burden and predicts memory decline. *eLife*. 2022;11:e78191. doi:10.7554/eLife.78191
34. Poisnel G, Arenaza-Urquijo E, Collette F, et al. The Age-Well randomized controlled trial of the Medit-Ageing European project: Effect of meditation or foreign language training on brain and mental health in older adults. *Alzheimer's & Dementia: Translational Research & Clinical Interventions*. 2018;4:714-723. doi:10.1016/j.trci.2018.10.011
35. Berry RB, Brooks R, Gamaldo C, et al. AASM Scoring Manual Updates for 2017 (Version 2.4). *Journal of Clinical Sleep Medicine*. 2017;13(05):665-666. doi:10.5664/jcsm.6576
36. Oostenveld R, Fries P, Maris E, Schoffelen JM. FieldTrip: Open Source Software for Advanced Analysis of MEG, EEG, and Invasive Electrophysiological Data. *Computational Intelligence and Neuroscience*. 2011;2011:1-9. doi:10.1155/2011/156869
37. Muehlroth BE, Werkle-Bergner M. Understanding the interplay of sleep and aging: Methodological challenges. *Psychophysiology*. 2020;57(3). doi:10.1111/psyp.13523

38. La Joie R, Perrotin A, de La Sayette V, et al. Hippocampal subfield volumetry in mild cognitive impairment, Alzheimer's disease and semantic dementia. *NeuroImage: Clinical*. 2013;3:155-162. doi:10.1016/j.nicl.2013.08.007
39. Landau SM, Fero A, Baker SL, et al. Measurement of longitudinal  $\beta$ -amyloid change with 18F-florbetapir PET and standardized uptake value ratios. *Journal of Nuclear Medicine*. 2015;56(4):567-574. doi:10.2967/jnumed.114.148981
40. Chen K, Roontiva A, Thiyyagura P, et al. Improved power for characterizing longitudinal amyloid- $\beta$  PET changes and evaluating amyloid-modifying treatments with a cerebral white matter reference region. *Journal of Nuclear Medicine*. 2015;56(4):560-566. doi:10.2967/jnumed.114.149732
41. Murphy M, Riedner BA, Huber R, Massimini M, Ferrarelli F, Tononi G. Source modeling sleep slow waves. *Proceedings of the National Academy of Sciences*. 2009;106(5):1608-1613. doi:10.1073/pnas.0807933106
42. Massimini M. The Sleep Slow Oscillation as a Traveling Wave. *Journal of Neuroscience*. 2004;24(31):6862-6870. doi:10.1523/JNEUROSCI.1318-04.2004
43. Marshall L, Helgadóttir H, Mölle M, Born J. Boosting slow oscillations during sleep potentiates memory. *Nature*. 2006;444(7119):610-613. doi:10.1038/nature05278
44. Taillard J, Sagaspe P, Berthomier C, et al. Non-REM Sleep Characteristics Predict Early Cognitive Impairment in an Aging Population. *Frontiers in Neurology*. 2019;10. doi:10.3389/fneur.2019.00197
45. Steriade M. Grouping of brain rhythms in corticothalamic systems. *Neuroscience*. 2006;137(4):1087-1106. doi:10.1016/j.neuroscience.2005.10.029
46. Achermann P, Borbély AA. Low-frequency (<1Hz) oscillations in the human sleep electroencephalogram. *Neuroscience*. 1997;81(1):213-222. doi:10.1016/S0306-4522(97)00186-3
47. Hubbard J, Gent TC, Hoekstra MMB, et al. Rapid fast-delta decay following prolonged wakefulness marks a phase of wake-inertia in NREM sleep. *Nat Commun*. 2020;11(1):3130. doi:10.1038/s41467-020-16915-0
48. Bersagliere A, Pascual-Marqui RD, Tarokh L, Achermann P. Mapping Slow Waves by EEG Topography and Source Localization: Effects of Sleep Deprivation. *Brain Topogr*. 2018;31(2):257-269. doi:10.1007/s10548-017-0595-6
49. Kastanenka KV, Calvo-Rodriguez M, Hou SS, et al. Frequency-dependent exacerbation of Alzheimer's disease neuropathophysiology. *Sci Rep*. 2019;9(1):8964. doi:10.1038/s41598-019-44964-z
50. Lee YF, Gerashchenko D, Timofeev I, Bacskai BJ, Kastanenka KV. Slow Wave Sleep Is a Promising Intervention Target for Alzheimer's Disease. *Frontiers in Neuroscience*. 2020;14. doi:10.3389/fnins.2020.00705

51. Spira AP, Gamaldo AA, An Y, et al. Self-Reported Sleep and  $\beta$ -Amyloid Deposition in Community-Dwelling Older Adults. *JAMA Neurol.* 2013;70(12):1537-1543. doi:10.1001/jamaneurol.2013.4258
52. Branger P, Arenaza-Urquijo EM, Tomadesso C, et al. Relationships between sleep quality and brain volume, metabolism, and amyloid deposition in late adulthood. *Neurobiology of Aging.* 2016;41:107-114. doi:10.1016/j.neurobiolaging.2016.02.009
53. Brown BM, Rainey-Smith SR, Villemagne VL, et al. The Relationship between Sleep Quality and Brain Amyloid Burden. *Sleep.* 2016;39(5):1063-1068. doi:10.5665/sleep.5756
54. Carvalho DZ, St Louis EK, Knopman DS, et al. Association of Excessive Daytime Sleepiness With Longitudinal  $\beta$ -Amyloid Accumulation in Elderly Persons Without Dementia. *JAMA Neurology.* 2018;75(6):672. doi:10.1001/jamaneurol.2018.0049
55. You JC, Jones E, Cross DE, et al. Association of  $\beta$ -Amyloid Burden With Sleep Dysfunction and Cognitive Impairment in Elderly Individuals With Cognitive Disorders. *JAMA Network Open.* 2019;2(10):e1913383-e1913383. doi:10.1001/jamanetworkopen.2019.13383
56. Du L, Langhough R, Hermann BP, et al. Associations between self-reported sleep patterns and health, cognition and amyloid measures: results from the Wisconsin Registry for Alzheimer's Prevention. *Brain Communications.* 2023;5(2):fcad039. doi:10.1093/braincomms/fcad039
57. Gabelle A, Gutierrez LA, Jaussent I, et al. Absence of Relationship Between Self-Reported Sleep Measures and Amyloid Load in Elderly Subjects. *Front Neurol.* 2019;10:989. doi:10.3389/fneur.2019.00989
58. Van Den Berg JF, Van Rooij FJA, Vos H, et al. Disagreement between subjective and actigraphic measures of sleep duration in a population-based study of elderly persons\*. *Journal of Sleep Research.* 2008;17(3):295-302. doi:10.1111/j.1365-2869.2008.00638.x
59. Landry G, Best J, Liu-Ambrose T. Measuring sleep quality in older adults: a comparison using subjective and objective methods. *Frontiers in Aging Neuroscience.* 2015;7:166. doi:10.3389/fnagi.2015.00166
60. Åkerstedt T, Schwarz J, Gruber G, Lindberg E, Theorell-Haglöw J. The relation between polysomnography and subjective sleep and its dependence on age – poor sleep may become good sleep. *Journal of Sleep Research.* 2016;25(5):565-570. doi:10.1111/jsr.12407
61. Lucey BP, Hicks TJ, McLeland JS, et al. Effect of sleep on overnight cerebrospinal fluid amyloid  $\beta$  kinetics: Disrupted Sleep and Amyloid  $\beta$ . *Ann Neurol.* 2018;83(1):197-204. doi:10.1002/ana.25117

62. Chylinski D, Van Egroo M, Narbutas J, et al. Heterogeneity in the links between sleep arousals, amyloid- $\beta$ , and cognition. *JCI Insight*. 2021;6(24):e152858. doi:10.1172/jci.insight.152858
63. André C, Rehel S, Kuhn E, et al. Association of Sleep-Disordered Breathing With Alzheimer Disease Biomarkers in Community-Dwelling Older Adults: A Secondary Analysis of a Randomized Clinical Trial. *JAMA Neurol*. 2020;77(6):716. doi:10.1001/jamaneurol.2020.0311
64. Baril AA, Martineau-Dussault MÈ, Sanchez E, et al. Obstructive Sleep Apnea and the Brain: a Focus on Gray and White Matter Structure. *Curr Neurol Neurosci Rep*. 2021;21(3):11. doi:10.1007/s11910-021-01094-2
65. Ancoli-Israel S, Ancoli-Israel S, Kripke DF, et al. Sleep-Disordered Breathing in Community-Dwelling Elderly. *Sleep*. 1991;14(6):486-495. doi:10.1093/sleep/14.6.486
66. Senaratna CV, Perret JL, Lodge CJ, et al. Prevalence of obstructive sleep apnea in the general population: A systematic review. *Sleep Medicine Reviews*. 2017;34:70-81. doi:10.1016/j.smr.2016.07.002

## List of figures

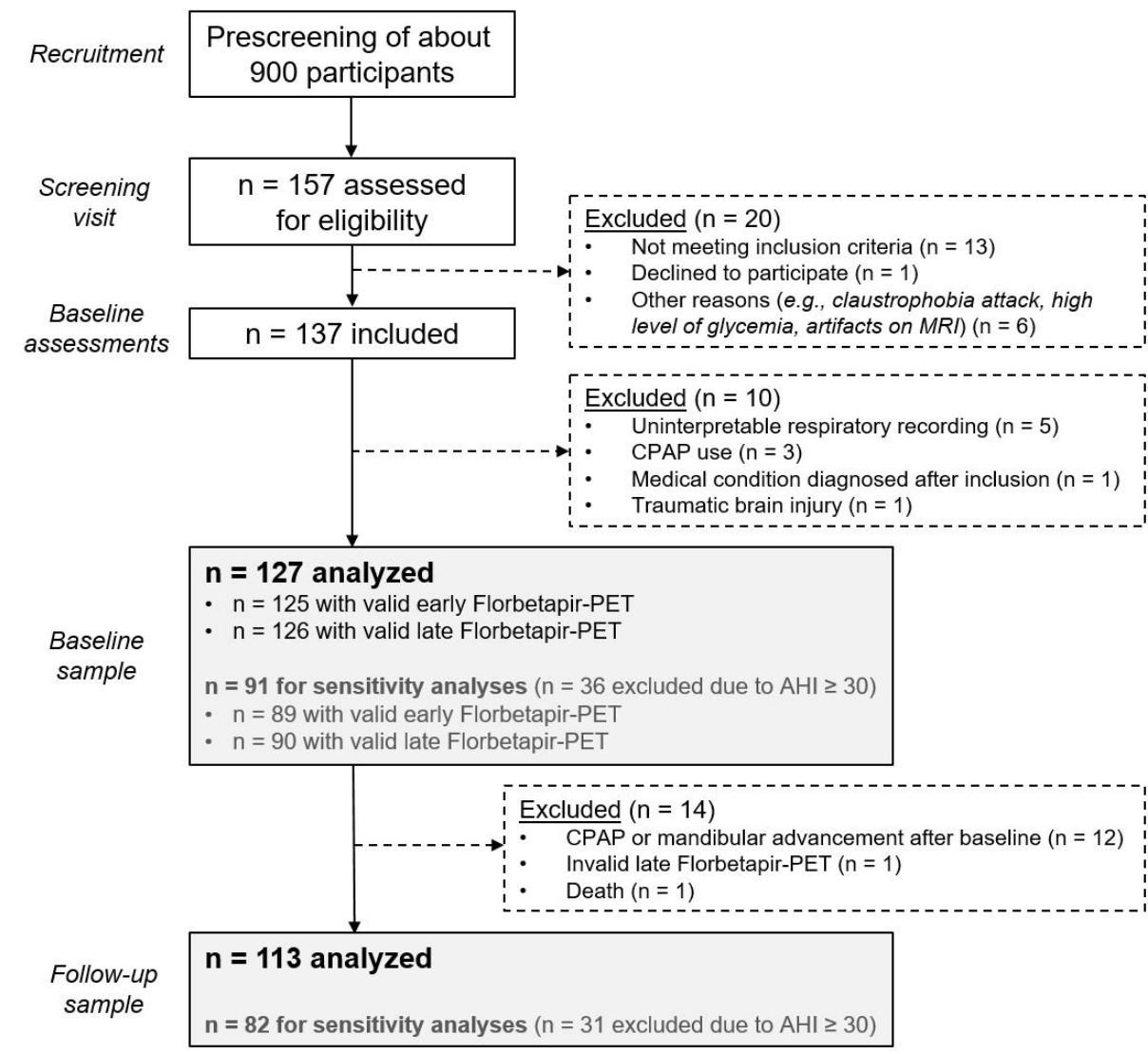


**Figure 1.** Flowchart of the inclusion process.

**Abbreviations:** *AHI* (Apnea-Hypopnea Index), *CPAP* (Continuous Positive Airway Pressure), *MRI* (Magnetic Resonance Imaging), *PAC* (Percent Annual Change), *PET* (Positron Emission Tomography).

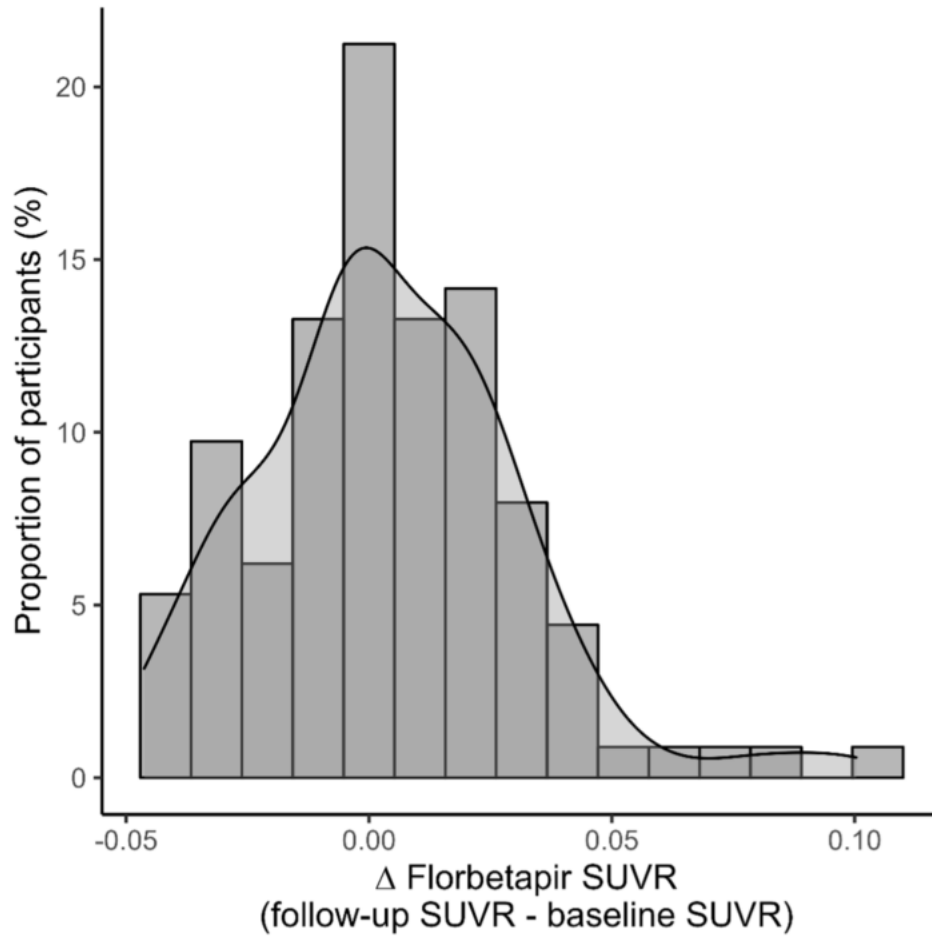


**Figure 2. Distribution of  $\Delta$  Florbetapir SUVR.**

*Histogram showing the distribution of  $\Delta$  Florbetapir SUVR reflecting global amyloid accumulation over the follow-up ( $20.7 \pm 0.9$  months) in the full sample ( $n = 113$ ). The curve represents the density of the distribution. Abbreviations: SUVR (Standard Uptake Value Ratios).*

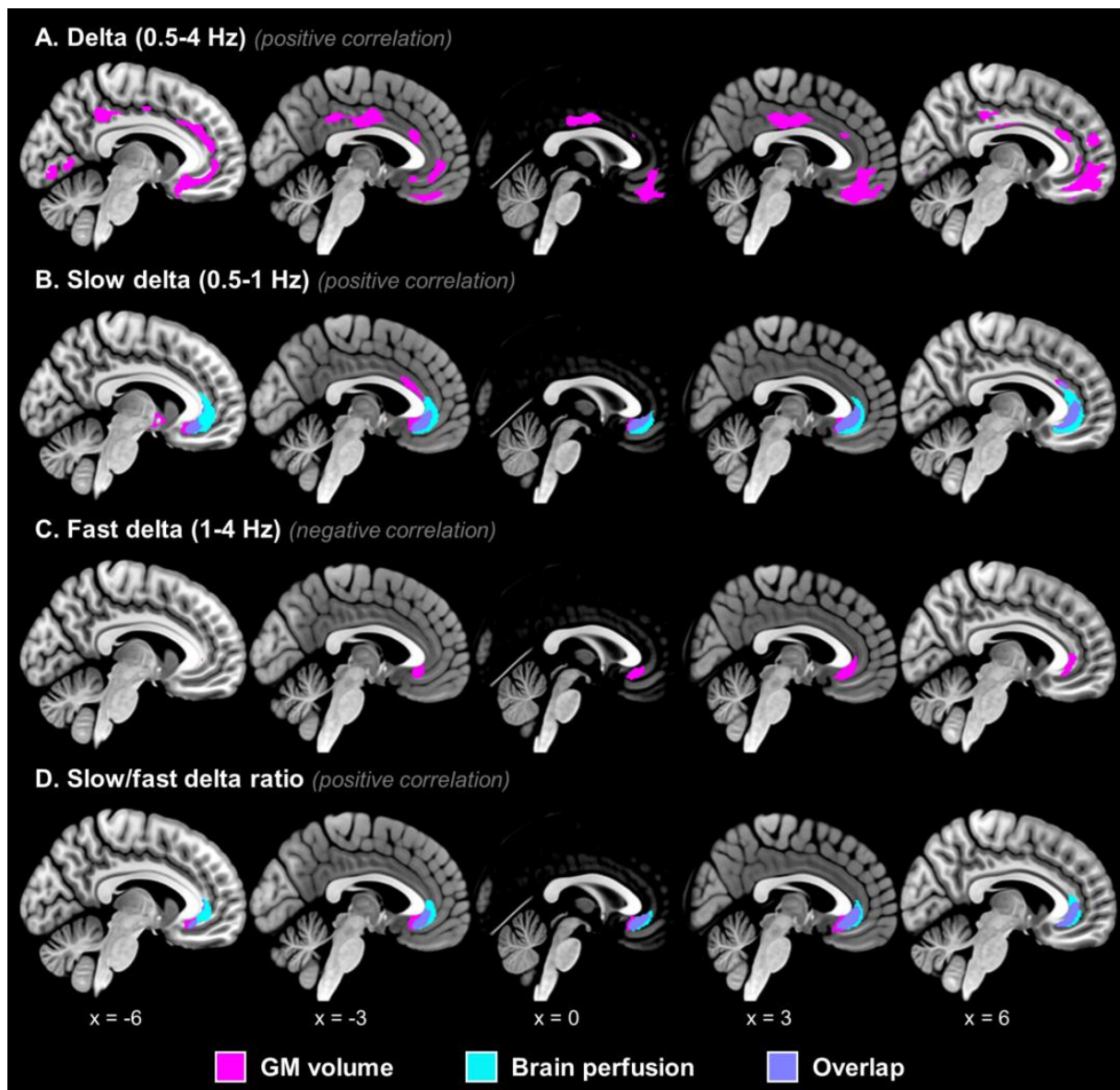
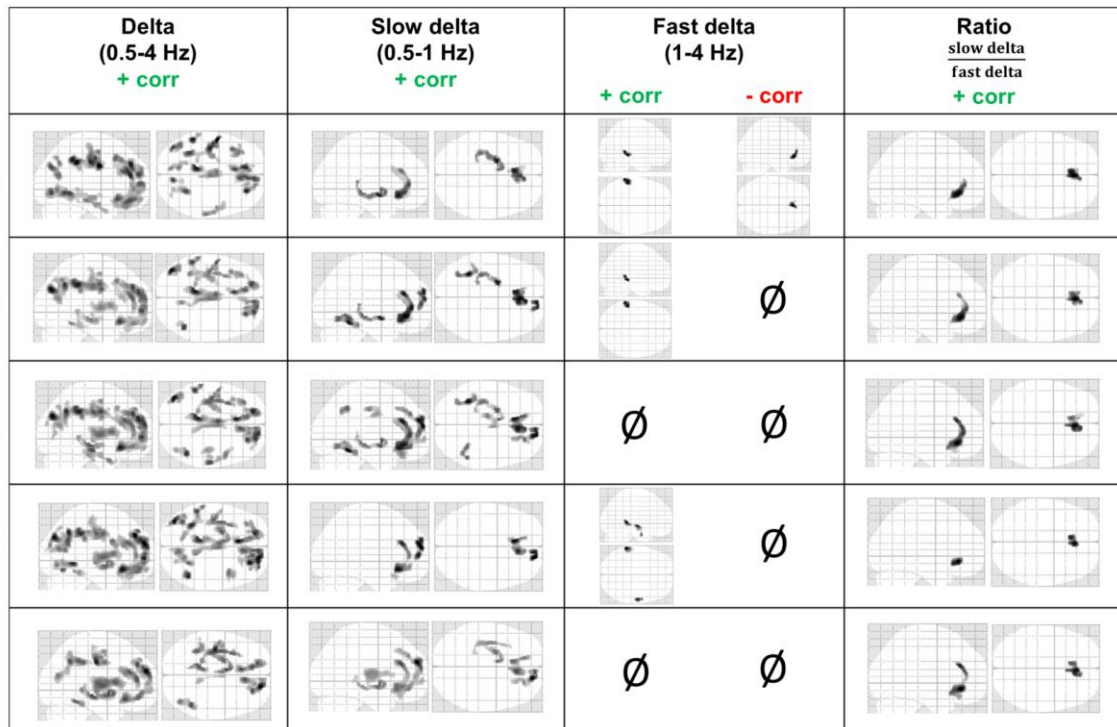


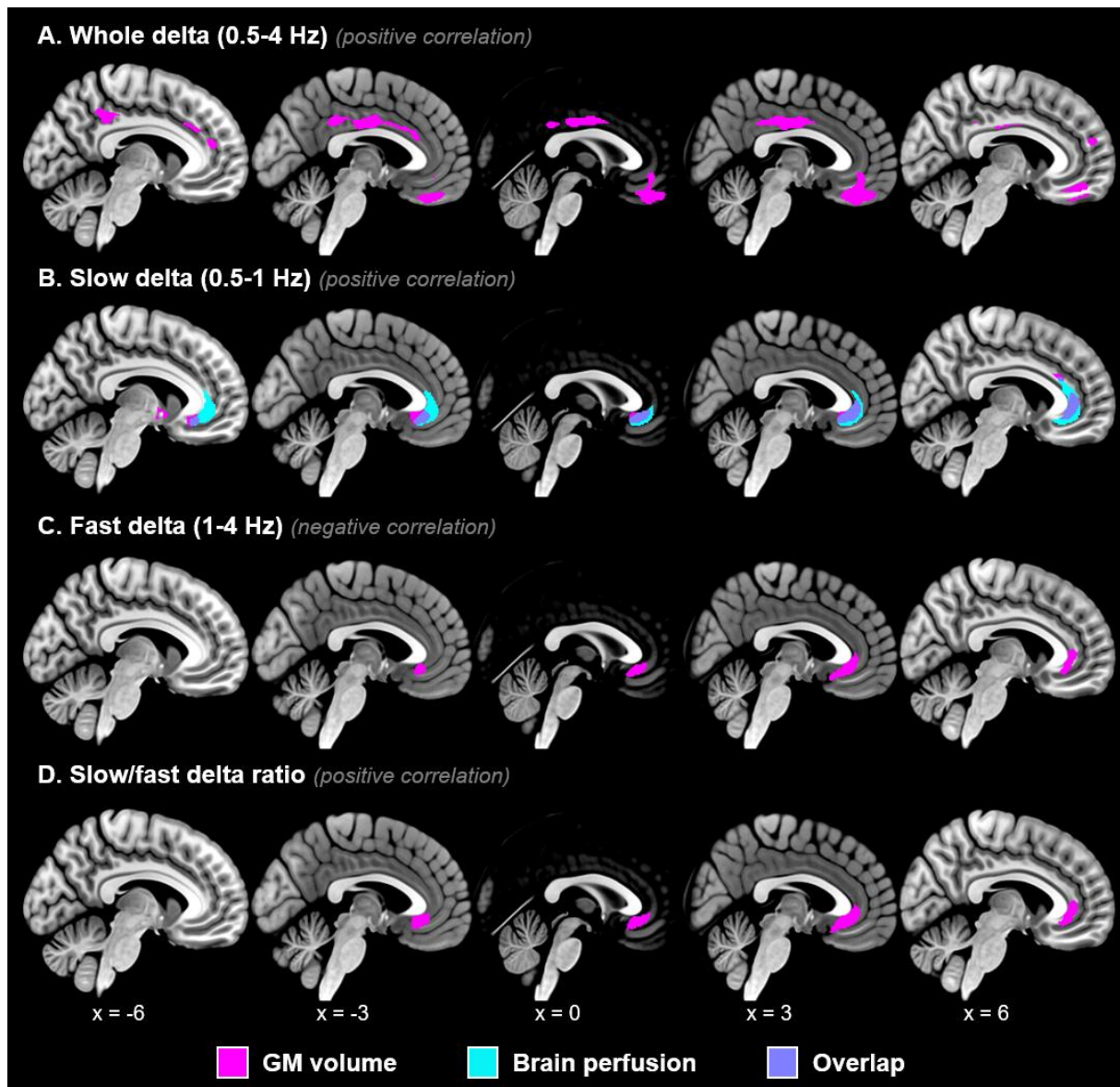
**Figure 3. Neuroimaging correlates of N2-N3 sleep delta power.**

Results of voxel-wise multiple regressions showing significant associations between frontal delta power during N2-N3 sleep and GM volume (magenta), brain perfusion (cyan), as well as their overlap (purple). No significant cluster was found with the amyloid burden or amyloid PAC (percent annual change). Results are presented at the  $p < 0.005$  (uncorrected) level combined with a minimum cluster size to achieve a corrected statistical significance of  $p < 0.05$  after controlling for age, sex, education, AHI and ApoE4 status (and intervention group for amyloid PAC). Coordinates are indicated in the MNI space.



**Supplementary Figure 1. Glassbrain projections of voxel-wise regressions between GM volume and N2-N3 sleep delta power calculated on different scalp regions.**

Results of voxel-wise multiple regressions showing significant associations between N2-N3 sleep delta power on several derivations and GM volume. All significant positive (+ corr, in green) and negative (-corr, in red) correlations are displayed (see Table 2). Results are presented at the  $p < 0.005$  (uncorrected) level combined with a minimum cluster size determined by Monte-Carlo simulations using the AlphaSim program to achieve a corrected statistical significance of  $p < 0.05$  after controlling for age, sex, education, AHI and ApoE4 status.



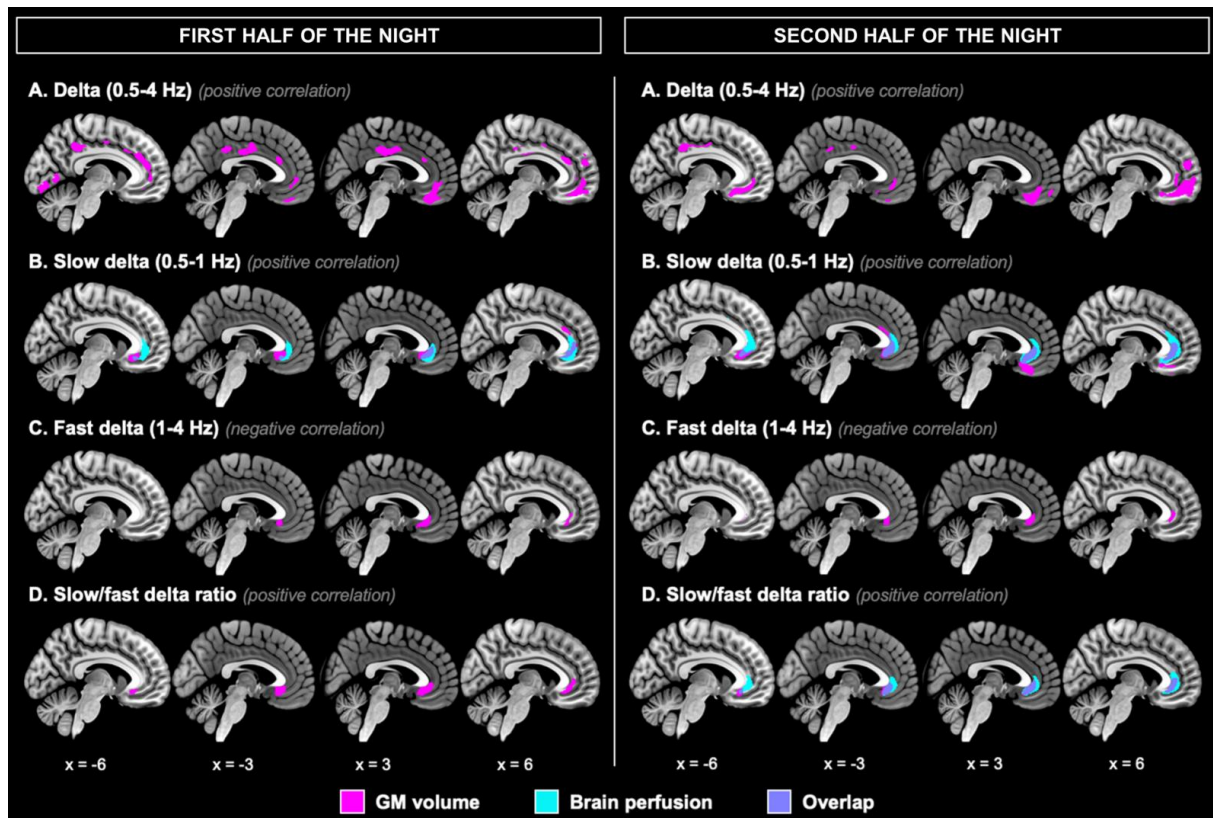
**Supplementary Figure 2. Neuroimaging correlates of N3 delta power.**

Results of voxel-wise multiple regressions showing significant associations between frontal delta power during N3 sleep and GM volume (magenta), brain perfusion (cyan), as well as their overlap (purple). No significant cluster was found with the amyloid burden or amyloid PAC (percent annual change). Results are presented at the  $p < 0.005$  (uncorrected) level combined with a minimum cluster size to achieve a corrected statistical significance of  $p < 0.05$  after controlling for age, sex, education, AHI and ApoE4 status (and intervention group for amyloid PAC). Coordinates are indicated in the MNI space. Two participants had no N3 epoch and were removed from this specific analysis.

	Delta (0.5-4 Hz) + corr	Slow delta (0.5-1 Hz) + corr	Fast delta (1-4 Hz) + corr      - corr	Ratio $\frac{\text{slow delta}}{\text{fast delta}}$ + corr
A. GM volume				
B. Brain perfusion	∅		∅	∅
C. Amyloid burden	∅	∅	∅	∅
D. Amyloid PAC	∅	∅	∅	∅

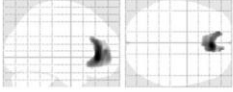
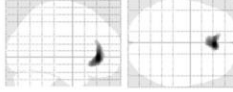
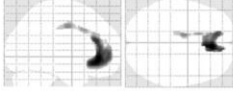
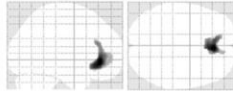
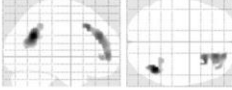
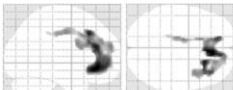
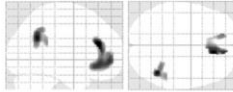
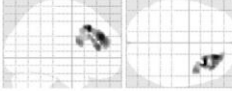
**Supplementary Figure 3. Glassbrain projections of voxel-wise regressions between neuroimaging and N2-N3 sleep delta power in participants without severe sleep apnea.**

Results of voxel-wise multiple regressions between frontal delta power during N2-N3 sleep and (A) GM volume, (B) brain perfusion, (C) amyloid burden and (D) amyloid PAC over time. All significant positive (+ corr, in green) and negative (- corr, in red) correlations are displayed (see Supplementary Table 3). Results are presented at the  $p < 0.005$  (uncorrected) level combined with a minimum cluster size determined by Monte-Carlo simulations using the AlphaSim program to achieve a corrected statistical significance of  $p < 0.05$  after controlling for age, sex, education, AHI and ApoE4 status (and intervention group for amyloid PAC).



**Supplementary Figure 4. Neuroimaging correlates delta power during N2-N3 epochs of the first and second half of the night.**

Results of voxel-wise multiple regressions showing significant associations between frontal delta power during N2-N3 epochs of the first (left panel) and the second (right panel) half of the night and GM volume (magenta), brain perfusion (cyan), as well as their overlap (purple). No significant cluster was found for amyloid burden or amyloid PAC (percent annual change). Results are presented at the  $p < 0.005$  (uncorrected) level combined with a minimum cluster size to achieve a corrected statistical significance of  $p < 0.05$  after controlling for age, sex, education, AHI and ApoE4 status (and intervention group for amyloid PAC). Coordinates are indicated in the MNI space.

	Delta (0.5-4 Hz) + corr	Slow delta (0.5-1 Hz) + corr	Fast delta (1-4 Hz) - corr	Ratio $\frac{\text{slow delta}}{\text{fast delta}}$ + corr
Frontal (F3, Fz, F4)	∅		∅	
Central (C3, Cz, C4)	∅		∅	
Parietal (P3, Pz, P4)			∅	∅
Temporal (T3, T4)	∅		∅	∅
Occipital (O1, O2)			∅	∅

**Supplementary Figure 5. Glassbrain projections of voxel-wise regressions between brain perfusion and N2-N3 sleep delta power calculated on different scalp regions.**

Results of voxel-wise multiple regressions between N2-N3 sleep delta power on several derivations and brain perfusion. All correlations were positive for delta, slow delta and ratio between slow and fast delta power (+ corr, in green) and negative for fast delta power (- corr, in red). Results are presented at the  $p < 0.005$  (uncorrected) level combined with a minimum cluster size determined by Monte-Carlo simulations using the AlphaSim program to achieve a corrected statistical significance of  $p < 0.05$ , after controlling for age, sex, education, AHI and ApoE4 status.

## List of Tables

**Table 1. Participant characteristics.**

Variable	Baseline (n = 127)	Follow-up (n = 113)
<b>Demographic</b>		
Age: years	69.0 ± 3.8	70.4 ± 3.8
Sex: nb (%) of women	80 (63.0)	71 (62.8)
Education: years	13.0 ± 3.1	13.3 ± 3.0
MMSE: total score	29.0 ± 1.0	-
GDS: total score	1.3 ± 1.8	1.6 ± 1.7
STAI-B: total score	34.5 ± 7.0	34.0 ± 8.0
BMI: kg/m <sup>2</sup>	26.2 ± 4.3	26.2 ± 4.7
Florbetapir SUVR*	1.24 ± 0.16	1.25 ± 0.17
Amyloid positive*: nb (%)	26 (20.6)	25 (22.1)
ApoE 4 carriers: nb (%)	34 (26.8)	30 (26.5)
<b>Sleep</b>		
Total sleep time: min	360.0 ± 64.6	-
Sleep efficiency: %	77.0 ± 10.0	-
Sleep latency: min	20.9 ± 13.8	-
WASO: min	87.0 ± 47.8	-
AHI: nb of events per hour	25.3 ± 14.8	-
N1 sleep: % of TST	13.6 ± 7.3	-
N2 sleep: % of TST	48.3 ± 8.8	-
N3 sleep: % of TST	19.8 ± 9.6	-
REM sleep: % of TST	18.3 ± 5.6	-

Data are presented as mean ± SD unless indicated otherwise. Of note, one participant had no N3 and was removed from the analyses for this specific sleep stage.

\*: missing data of late PET acquisition at baseline for one participant.

**Abbreviations:** AHI (Apnea-Hypopnea Index), ApoE (Apolipoprotein E), BMI (Body Mass Index), GDS (Geriatric Depression Scale), MMSE (Mini-Mental State Examination), nb (number), SD (Standard Deviation), SUVR (Standard Uptake Value Ratio, with cerebellum GM reference), TST (Total Sleep Time), WASO (wake after sleep onset).

**Table 2. Results of voxel-wise multiple regression analyses between neuroimaging data and frontal delta power during N2-N3 sleep.**

Frequency band	Corr	Brain areas	Cluster extent		MNI coordinates			T-values
			Nb of voxels	mm <sup>3</sup>	x	y	z	
<b>GM volume</b>								
Delta (0.5-4 Hz)	+	L pre and post central gyri	979	3304	-52	-4	32	5.09
		L middle cingulate cortex	1034	3490	-9	-39	36	5.02
		L inferior parietal lobule	313	1056	-52	-44	39	4.81
		R middle frontal gyrus	857	2892	27	42	33	4.76
		L ACC	769	2595	-8	40	18	4.62
		R lingual gyrus	652	2201	10	-75	-6	4.32
		L fusiform gyrus and L hippocampus	793	2676	-32	-50	-8	4.29
		L middle occipital and temporal gyri	645	2177	-39	-76	30	4.26
		B mOFC, R rectus and L ACC	1968	6642	-6	21	-15	4.24
		L middle frontal gyrus	447	1509	-38	20	44	3.94
		L lingual gyrus	452	1526	-8	-68	-2	3.67
		R middle and inferior temporal gyrus	338	1141	63	-24	-16	3.66
		Slow delta (0.5-1 Hz)	+	L hippocampus and L amygdala	597	2015	-18	-2
B ACC and mOFC	1191			4020	-4	26	-10	4.28
Fast delta (1-4 Hz)	+	L temporal middle gyrus	414	1397	-52	-33	-4	3.92
		- B ACC and mOFC	352	1188	3	32	-8	3.59
Ratio $\frac{\text{slow delta}}{\text{fast delta}}$	+	B ACC and mOFC	723	2440	3	32	-8	4.07
<b>Brain perfusion</b>								
Slow delta (0.5-1 Hz)	+	B ACC and mOFC	2806	9470	6	38	-2	3.96
Ratio $\frac{\text{slow delta}}{\text{fast delta}}$	+	B ACC and mOFC	1119	3777	4	36	-3	3.54

*T-values and MNI coordinates are indicated for the peak of each cluster. Cluster p-values are presented at the  $p < 0.005$  (uncorrected) level combined with a minimum cluster size to achieve a corrected statistical significance of  $p < 0.05$  after controlling for age, sex, education, AHI and ApoE4 status.*

*Abbreviations: ACC (Anterior Cingulate Cortex), AHI (Apnea-Hypopnea Index), ApoE (Apolipoprotein E), B (bilateral), corr (correlation), L (left), MNI (Montreal Neurological Institute), mOFC (medial OrbitoFrontal Cortex), R (Right), + (positive correlation), - (negative correlation).*

**Supplementary Table 1. Demographic characteristics and comparison of participants with and without severe sleep apnea.**

Variables	AHI < 30 subgroup (n = 91)	AHI ≥ 30 subgroup (n = 36)	Effect size	pvalue
Age: years	68.7 ± 3.3	69.7 ± 4.8	0.257 <sup>†</sup>	0.269
Sex: nb (%) of women	63 (69.2)	17 (47.2)	<b>2.51<sup>‡</sup></b>	<b>0.035</b>
Education: years	13.1 ± 3.2	12.7 ± 2.8	0.126 <sup>†</sup>	0.498
MMSE: total score	29.1 ± 1.0	28.8 ± 1.1	0.341 <sup>†</sup>	0.110
GDS: total score	1.3 ± 1.9	1.1 ± 1.2	0.146 <sup>†</sup>	0.374
STAI-B: total score	34.7 ± 7.2	34.1 ± 6.6	0.085 <sup>†</sup>	0.652
BMI: kg/m <sup>2</sup>	26.0 ± 4.5	26.6 ± 3.7	0.130 <sup>†</sup>	0.474
Florbetapir SUVR <sup>*</sup>	1.23 ± 0.14	1.28 ± 0.19	0.289 <sup>†</sup>	0.207
Amyloid positive <sup>*</sup> : nb (%)	16 (17.8)	10 (27.8)	0.56 <sup>‡</sup>	0.313
ApoE 4 carriers: nb (%)	23 (25.3)	11 (30.6)	0.77 <sup>‡</sup>	0.701

Data are presented as mean ± SD unless indicated otherwise. Effect sizes were estimated with Cohen's  $d^{\dagger}$  for continuous variables and with odd-ratio<sup>‡</sup> for categorical variables.

<sup>\*</sup>: missing data of late PET acquisition at baseline for one participant.

Abbreviations: ApoE (Apolipoprotein E), BMI (Body Mass Index), GDS (Geriatric Depression Scale), MMSE (Mini-Mental State Examination), nb (number), SD (Standard Deviation), SUVR (Standard Uptake Value Ratio, with cerebellum GM reference).

**Supplementary Table 2. Determination of minimal cluster sizes for each neuroimaging analyses.**

		GM volume	Brain perfusion	Baseline Amyloid burden	Amyloid PAC	
Full sample	<b>EEG power during N2-N3 sleep</b>					
	<b>Frontal EEG channels</b>					
	Delta	291	938	2553	57	
	Slow delta	293	1025	2578	55	
	Fast delta	262	1089	2630	54	
	Ratio slow delta/fast delta	264	1015	2402	61	
	<b>Central EEG channels</b>					
	Delta	297	888	2621	57	
	Slow delta	260	970	2429	57	
	Fast delta	267	978	2723	60	
	Ratio slow delta/fast delta	266	913	2491	58	
	<b>Parietal EEG channels</b>					
	Delta	297	961	2755	56	
	Slow delta	264	903	2431	57	
	Fast delta	304	1113	2746	60	
	Ratio slow delta/fast delta	267	1133	2648	63	
	<b>Temporal EEG channels</b>					
	Delta	250	892	2617	57	
	Slow delta	297	907	2549	55	
	Fast delta	267	952	2558	55	
	Ratio slow delta/fast delta	259	911	2737	62	
	<b>Occipital EEG channels</b>					
	Delta	259	1128	2560	60	
	Slow delta	268	928	2570	60	
	Fast delta	298	924	2767	56	
	Ratio slow delta/fast delta	263	1058	2669	55	
	Subgroup of participants without severe sleep apnea	<b>EEG power during N2-N3 sleep</b>				
		<b>Frontal EEG channels</b>				
Delta		245	905	2606	59	
Slow delta		302	1137	2522	53	
Fast delta		302	1137	2444	55	
Ratio slow delta/fast delta		306	1005	2419	59	

For each multiple regression analysis, minimal cluster size ( $k$  voxels) was determined using AlphaSim program, in order to achieve a corrected statistical significance of  $p < 0.05$ .

Abbreviations: GM (Gray Matter), PAC (Percent Annual Change).

**Supplementary Table 3. Results of voxel-wise multiple regression analyses between neuroimaging data and frontal delta power during N3 sleep.**

Frequency band	Corr	Brain areas	Cluster extent		MNI coordinates			T-values
			Nb of voxels	mm <sup>3</sup>	x	y	z	
<b>GM volume</b>								
Delta (0.5-4 Hz)	+	L inferior parietal cortex	266	898	-33	-48	40	4.66
		L superior frontal gyrus	247	834	-18	22	54	4.51
		L middle cingulate cortex	1237	4175	-8	-38	36	4.41
		L middle frontal gyrus	268	905	-36	20	42	4.22
		L middle temporal and occipital gyri, angular gyrus	557	1880	-42	-64	18	4.15
		B rectus and mOFC	621	2096	3	34	-24	4.00
		L pre and post central gyri	368	1242	-50	-6	32	3.98
		L lingual and fusiform gyri	334	1127	-30	-54	-6	3.89
		R frontal superior gyrus	473	1596	27	42	32	3.82
		L hippocampus	545	1839	-28	-15	-14	3.76
		R lingual and fusiform gyri	503	1698	27	-56	-9	3.60
Slow delta (0.5-1 Hz)	+	L hippocampus and amygdala	527	1779	-18	-2	-10	4.33
		R hippocampus, amygdala and putamen	638	2153	34	-20	-12	3.88
		B ACC and mOFC	728	2457	3	33	-8	3.85
Fast delta (1-4 Hz)	+	L temporal middle gyrus	430	1451	-54	-33	-4	3.86
		- B ACC and R mOFC	399	1347	3	32	-8	3.59
Ratio $\frac{\text{slow delta}}{\text{fast delta}}$	+	B ACC and mOFC	566	1910	3	33	-8	3.93
<b>Brain perfusion</b>								
Slow delta (0.5-1 Hz)	+	B ACC and mOFC	1777	5997	8	38	4	3.54

*T-values and MNI coordinates are indicated for the peak of each cluster. Cluster p-values are presented at the  $p < 0.005$  (uncorrected) level combined with a minimum cluster size to achieve a corrected statistical significance of  $p < 0.05$  after controlling for age, sex, education, AHI and ApoE4 status.*

*Abbreviations: ACC (Anterior Cingulate Cortex), AHI (Apnea-Hypopnea Index), ApoE (Apolipoprotein E), B (bilateral), corr (correlation), L (left), MNI (Montreal Neurological Institute), mOFC (medial OrbitoFrontal Cortex), R (Right), + (positive correlation), - (negative correlation).*

STROBE Statement—checklist of items that should be included in reports of observational studies

Manuscript Number: **Multimodal neuroimaging correlates of spectral power in NREM sleep delta sub-bands in cognitively unimpaired older adults**

	Item No	Recommendation	Indicate page number (or n/a if not applicable)
Title and abstract	1	(a) Indicate the study’s design with a commonly used term in the title or the abstract	Not done as the effect of the intervention is not tested in the present study.
		(b) Provide in the abstract an informative and balanced summary of what was done and what was found	2
<b>Introduction</b>			
Background/rationale	2	Explain the scientific background and rationale for the investigation being reported	4, 5
Objectives	3	State specific objectives, including any prespecified hypotheses	5
<b>Methods</b>			
Study design	4	Present key elements of study design early in the paper	5-11
Setting	5	Describe the setting, locations, and relevant dates, including periods of recruitment, exposure, follow-up, and data collection	5, 6, 8
Participants	6	(a) Cohort study—Give the eligibility criteria, and the sources and methods of selection of participants. Describe methods of follow-up	5, 6; Fig. 1 and see Poisnel et al. (2018) describing the Age-Well randomized controlled trial
		Case-control study—Give the eligibility criteria, and the sources and methods of case ascertainment and control selection. Give the rationale for the choice of cases and controls	n/a
		Cross-sectional study—Give the eligibility criteria, and the sources and methods of selection of participants	5, 6; Fig. 1 and see Poisnel et al. (2018) describing the Age-Well randomized controlled trial
		(b) Cohort study—For matched studies, give matching criteria and number of exposed and unexposed	n/a

		Case-control study—For matched studies, give matching criteria and the number of controls per case	n/a
Variables	7	Clearly define all outcomes, exposures, predictors, potential confounders, and effect modifiers. Give diagnostic criteria, if applicable	6-11
Data sources/ measurement	8*	For each variable of interest, give sources of data and details of methods of assessment (measurement). Describe comparability of assessment methods if there is more than one group	6-11
Bias	9	Describe any efforts to address potential sources of bias	10, 11
Study size	10	Explain how the study size was arrived at	The sample size has been calculated for another primary outcome (see Poisnel et al. (2018) describing the Age-Well randomized controlled trial and Chételat et. (2022) for the primary outcome paper).
Quantitative variables	11	Explain how quantitative variables were handled in the analyses. If applicable, describe which groupings were chosen and why	6-11
Statistical methods	12	(a) Describe all statistical methods, including those used to control for confounding	10, 11
		(b) Describe any methods used to examine subgroups and interactions	10, 11
		(c) Explain how missing data were addressed	n/a
		(d) Cohort study—If applicable, explain how loss to follow-up was addressed	Figure 1
		Case-control study—If applicable, explain how matching of cases and controls was addressed	n/a
		Cross-sectional study—If applicable, describe analytical methods taking account of sampling strategy	n/a
		(e) Describe any sensitivity analyses	10, 11
<b>Results</b>			
Participants	13*	(a) Report numbers of individuals at each stage of study—eg numbers potentially eligible, examined for eligibility, confirmed eligible, included in the study, completing follow-up, and analysed	11, Fig. 1
		(b) Give reasons for non-participation at each stage	Fig. 1
		(c) Consider use of a flow diagram	Fig. 1

		(a) Give characteristics of study participants (eg demographic, clinical, social) and information on exposures and potential confounders	5, 6, 11; Table 1; Supplementary Table 1
Descriptive data	14*	(b) Indicate number of participants with missing data for each variable of interest	8; Table 1; Supplementary Table 1
		(c) Cohort study—Summarise follow-up time (eg, average and total amount)	11
		Cohort study—Report numbers of outcome events or summary measures over time	Table 1; Figure 2
Outcome data	15*	Case-control study—Report numbers in each exposure category, or summary measures of exposure	n/a
		Cross-sectional study—Report numbers of outcome events or summary measures	n/a
		(a) Give unadjusted estimates and, if applicable, confounder-adjusted estimates and their precision (eg, 95% confidence interval). Make clear which confounders were adjusted for and why they were included	12, 13; Tables 2; Fig. 3
Main results	16	(b) Report category boundaries when continuous variables were categorized	n/a
		(c) If relevant, consider translating estimates of relative risk into absolute risk for a meaningful time period	n/a
		Report other analyses done—eg analyses of subgroups and interactions, and sensitivity analyses	12, 13; Supplementary Table 3; Supplementary Fig.1-4
<b>Discussion</b>			
Key results	18	Summarise key results with reference to study objectives	14
Limitations	19	Discuss limitations of the study, taking into account sources of potential bias or imprecision. Discuss both direction and magnitude of any potential bias	17
Interpretation	20	Give a cautious overall interpretation of results considering objectives, limitations, multiplicity of analyses, results from similar studies, and other relevant evidence	14-17
Generalisability	21	Discuss the generalisability (external validity) of the study results	17, 18
<b>Other information</b>			
Funding	22	Give the source of funding and the role of the funders for the present study and, if applicable, for the original study on which the present article is based	19, 20

